

Integrating Silicon Nanowire Field Effect Transistor, Microfluidics and Air Sampling Techniques For Real-Time Monitoring Biological Aerosols

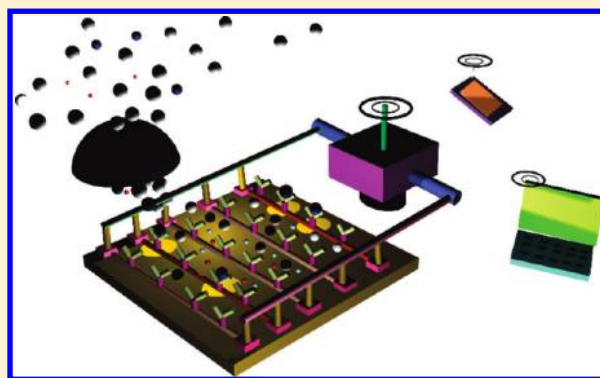
Fangxia Shen,[†] Miaomiao Tan,[†] Zhenxing Wang,[‡] Maosheng Yao,^{†,*} Zhenqiang Xu,[†] Yan Wu,[†] Jindong Wang,[‡] Xuefeng Guo,^{‡,*} and Tong Zhu^{†,*}

[†]State Key Joint Laboratory of Environmental Simulation and Pollution Control, College of Environmental Sciences and Engineering, Peking University, Beijing 100871, China

[‡]Beijing National Laboratory for Molecular Sciences, State Key Laboratory for Structural Chemistry of Unstable and Stable Species, College of Chemistry and Molecular Engineering, Peking University, Beijing 100871, China

S Supporting Information

ABSTRACT: Numerous threats from biological aerosol exposures, such as those from H1N1 influenza, SARS, bird flu, and bioterrorism activities necessitate the development of a real-time bioaerosol sensing system, which however is a long-standing challenge in the field. Here, we developed a real-time monitoring system for airborne influenza H3N2 viruses by integrating electronically addressable silicon nanowire (SiNW) sensor devices, microfluidics and bioaerosol-to-hydrosol air sampling techniques. When airborne influenza H3N2 virus samples were collected and delivered to antibody-modified SiNW devices, discrete nanowire conductance changes were observed within seconds. In contrast, the conductance levels remained relatively unchanged when indoor air or clean air samples were delivered. A 10-fold increase in virus concentration was found to give rise to about 20–30% increase in the sensor response. The selectivity of the sensing device was successfully demonstrated using H1N1 viruses and house dust allergens. From the simulated aerosol release to the detection, we observed a time scale of 1–2 min. Quantitative polymerase chain reaction (qPCR) tests revealed that higher virus concentrations in the air samples generally corresponded to higher conductance levels in the SiNW devices. In addition, the display of detection data on remote platforms such as cell phone and computer was also successfully demonstrated with a wireless module. The work here is expected to lead to innovative methods for biological aerosol monitoring, and further improvements in each of the integrated elements could extend the system to real world applications.



INTRODUCTION

The biological aerosol (bioaerosol) exposures such as those from H1N1 influenza, SARS,¹ bird flu² outbreaks, and also bioterrorism³ events have resulted in grave human and economic costs. Additionally, increasing level of international travel also enhances the possibility of allowing an infectious disease to quickly develop into a possible pandemic. These threats necessitate the development of a real-time bioaerosol sensing system, which however is a long-standing challenge in the field. Some technologies, for example, bioaerosol mass spectrometry (BAMS),⁴ surface-enhanced Raman spectroscopy (SERS),⁵ flow cytometry with fluorochrome,⁶ and other fluorescence based technologies such as ultraviolet aerodynamic particle sizer (UVAPS)^{7,8} have been investigated or adapted for possible detection of airborne biological agents in a real-time manner. Unfortunately, most of these techniques are incapable of species level discrimination and/or have high false alarm rates.

With an advanced bioaerosol sampling system, qPCR, PCR, and RT-PCR can identify species with improvements of detection

limits of bioagents in the air samples, but they are difficult to be automated as an unattended bioaerosol sensing system. For instance, the preparation of DNA sample is a labor-intensive and tedious procedure, and the detection time could be up to several hours. This is far away from the objective of “detect-to-warn” time span, which is generally agreed as 1 min to allow a timely response or rescue in a man-made bioterror event.⁹ In addition, these techniques are incapable of differentiating between dead and live cells. Use of the UVAPS can yield the total viable bioaerosol concentrations in a real-time manner based on the fluorescence emitted from reduced pyridine nucleotides (e.g., NAD(P)H) and riboflavin) associated with viable particles, but its major drawback is its inability for species level discrimination.^{7,8,10} For bioaerosol mass spectrometry, the background noise and

Received: December 28, 2010

Accepted: July 22, 2011

Revised: July 11, 2011

Published: July 22, 2011

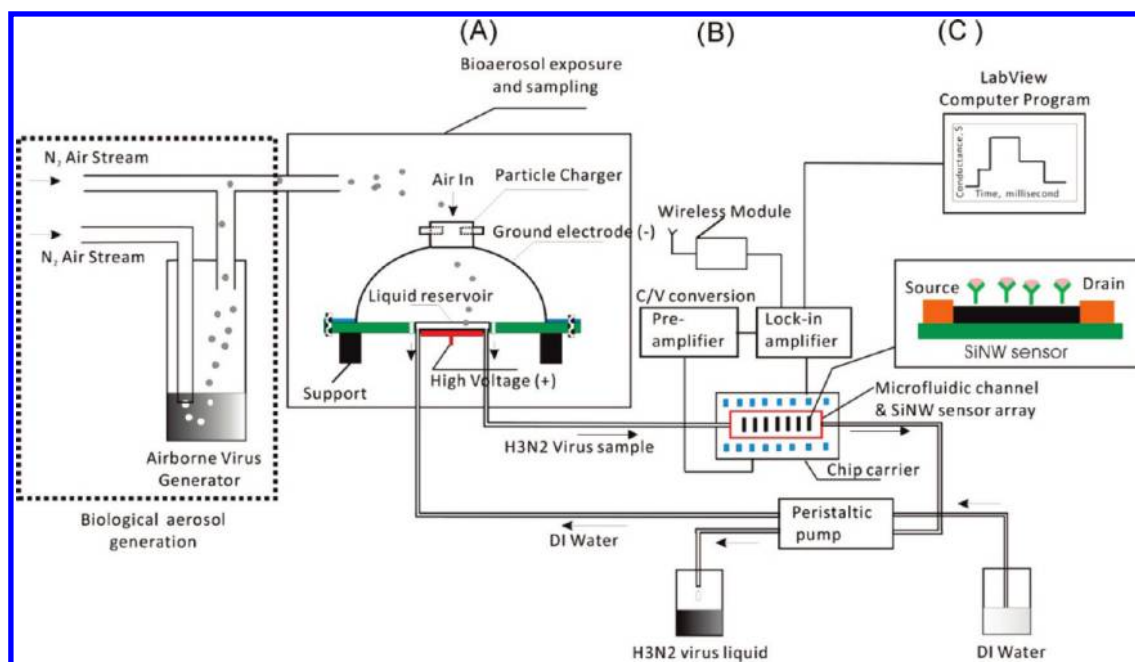


Figure 1. Sketch of experimental setup for real-time detection of airborne influenza H3N2 viruses using silicon nanowire field effect transistor (SiNW-FET); the system is composed of three major parts: (A) bioaerosol sampling and delivery, (B) antibody modified silicon nanowire based biosensor, and (C) signal amplification, detection, and online monitoring. Wireless module is shown in SI Figure S4; Fresh DI water was continuously refilled into the liquid reservoir through a peristaltic pump; For testing the system, airborne influenza A viruses were aerosolized using a Collison Nebulizer.

analysis of multiple spectra peaks contribute to the high false alarm rates,⁴ thus affecting its use in practical environments. Apparently, updated versions or a new type of real-time bioaerosol detection technology is in great need.

Recently, label-free silicon nanowire (SiNW) has been successfully applied to the detection of biological species in liquids through translating molecular binding events into microelectronic signals via field-effect transistor (FET).^{11–13} This development creates a bridge between different disciplines, presenting an outstanding opportunity for its environmental sensing applications.¹⁴ In the meantime, advances in microfluidic channels¹⁵ have enabled the efficient transport of minute amounts of virus-laden liquids onto specific antibody-coated multiplexed FETs constructed using silicon nanowires.^{12,13} If such a combination is attempted for airborne bioaerosol exposure monitoring, a technology that is able to efficiently translate bioaerosols into hydrosols without damaging their biological integrity is needed. Unfortunately, investigators in different fields often diverge without knowing these preexisting technologies.¹⁴

Here, we reported the integration of silicon nanowire field effect transistor (SiNW FET), microfluidics and air sampling techniques for label-free real-time monitoring of biological aerosols. In investigating such feasibility, we first designed and built an electrostatic air sampling system that can transfer airborne virus particles into small amounts of liquids. Second, we fabricated nanowire sensor devices and applied both microfluidic channel and peristaltic pump to deliver the collected airborne viruses for sensing. The biological aerosol detection events were recorded in a real-time manner using electrical signal amplifiers. The virus concentrations in the collected air samples (used for the nanowire sensing) were also quantified using qPCR. The

work here is expected to lead to innovative methods for biological aerosol monitoring.

■ MATERIALS AND METHODS

Experimental Setup. The label-free real-time bioaerosol detection system developed in this study is shown in Figure 1, excluding the bioaerosol generation part. The system is composed of three major parts: (A) bioaerosol sampling and delivery, (B) antibody modified silicon nanowire based biosensor, and (C) signal amplification, detection, and online monitoring. For testing the system, airborne H3N2 influenza viruses were produced using a Collison nebulizer (BGI, Waltham, MA). For bioaerosol sampling, a new electrostatic air sampler was designed using a half-ball shape steel electrode (radius is 45 mm) with three aerosol inlets on the top and a copper plate electrode (16 mm in diameter) suited inside a circular plastic support. Above the plate electrode, a plastic cylindrical reservoir (14 mm in diameter and 1 mm in height) was built with a liquid inlet and a liquid outlet made of copper (2 mm in diameter).²¹ These outlets are connected to a peristaltic pump for the liquid delivery. Next to the reservoir, there are two aerosol outlets connected to a vacuum pump. The investigation of its physical and biological collection efficiencies were performed in another study.²¹ In this study, silicon nanowires were prepared using the chemical vapor deposition (CVD) method as described in the Supporting Information (SI); the field effect transistor biosensor was constructed as described in the SI. The electrical properties of representative silicon nanowire sensor devices were analyzed using a semiconductor property analyzer (4156C, Agilent). An example of the sensor's current vs gate voltage curve was presented in SI Figure S1. A preamplifier (LI-76, NF Corporation) and a lock-in amplifier (LI S640, NF

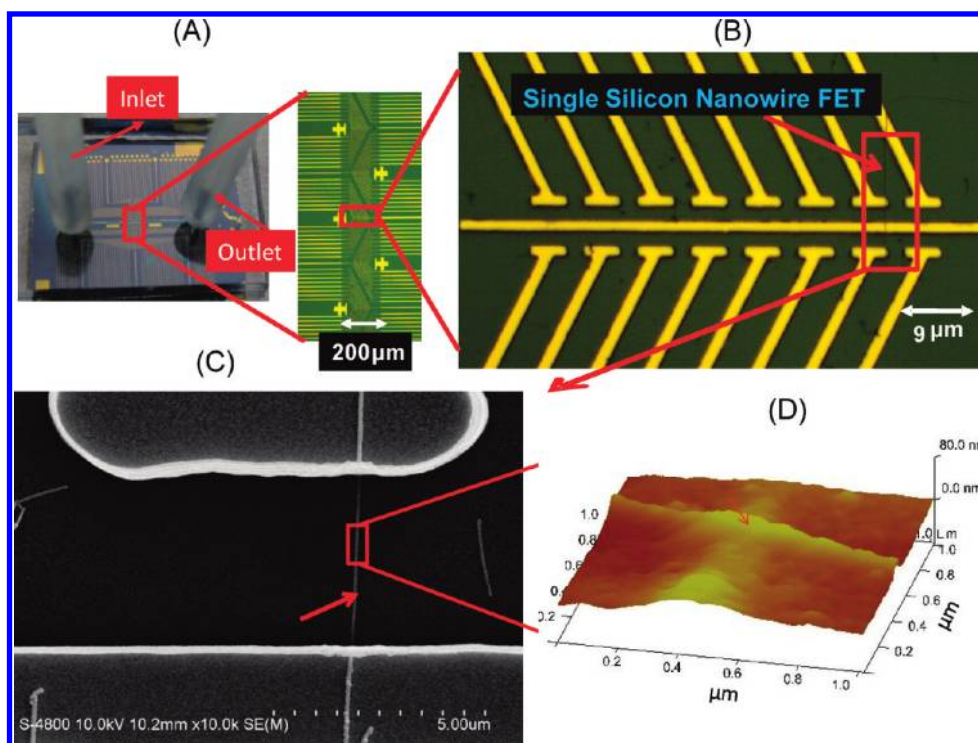


Figure 2. Representative optical images of silicon nanowire (SiNW) chip and microfluidic channel: (A) SiNW sensor array with PDMS microfluidic channel with an inlet and an outlet fabricated here, (B) magnified part (red rectangle in (A)) of the SiNW sensor device, (C) Scanning Electron Microscopy (SEM) images of single silicon nanowire FET pointed by an arrow shown in (B); PDMS microfluidic channel was fabricated using the procedures described in the SI; (D) Atomic force microscopy of an antibody modified silicon nanowire.

Corporation) were connected to the electrodes of the sensor devices. The PDMS channel was fabricated by the procedure as described in the SI and placed on the sensor chip covering the entire nanowire sensor area ($\sim 4 \mu\text{m}$ wide) as shown in Figure 2 (A). Before the experiments, the nanowire sensing devices were further functionalized using influenza A H3N2 subtype antibodies (Abcam Ltd., HKSTP, N.T. Hong Kong) following the procedures shown in SI Figure S2. Representative optical images of silicon nanowire (SiNW) devices used in this study were shown in Figure 2 (B, C). Figure 2 (D) shows the three-dimensional image obtained by an atomic force microscope for the antibody coated silicon nanowire, and the arrow in the figure indicates the spot where the antibody is linked to the nanowire.

Airborne Virus Sensing Experiments Using Silicon Nanowire Sensor Devices. Influenza A H3N2 virus samples (inactivated) were received from Jiangsu Center for Diseases Prevention and Control (Jiangsu, China) and used as it was. When performing the experiments, the virus particles were aerosolized as shown in Figure 1 using an aerosol generator, Collision nebulizer (BGI Inc., Waltham, MA) at an aerosolization rate of 2.5 L/min of nitrogen gas, and the airborne viruses were further carried into the chamber by a flow rate of 13 L/min of nitrogen gas. The electrostatic sampler was connected to a high voltage supply (model 205B-15R from Bertan Associate, Inc., Valhalla, NY), and different voltages were applied for the sensing experiments (0, 5, 10, 20 kV). The air samples were collected at a sampling flow rate of 5 L/min in this study. Through a peristaltic pump, the H3N2 virus aerosol samples collected into the liquid reservoir shown in Figure 1 were continuously transported to the functional nanowire sensing device via an inlet and an outlet in

the polydimethylsiloxane (PDMS) channel shown in Figure 2 (A). The nanowire conductance data vs time were recorded using a preamplifier (LI-76, NF Corporation) and a lock-in amplifier (LI 5640, NF Corporation), and displayed in a real-time manner using a LabView computer program as shown in Figure 1. The lock-in amplifier was operated with a modulation frequency of 79 Hz, and the preamplifier had a current/voltage gain factor of 10^4 . The modulation amplitude was 50 mV and the dc source-drain potential was zeroed to avoid electrochemical reactions. The virus sensing was performed by either adding $5 \mu\text{L}$ virus samples directly onto the sensor or delivering the collected samples continuously into the microfluidic channel at a flow rate of 0.4 mL/min through the peristaltic pump during the sensing experiments. Following the same procedure, some of the sensing selectivity experiments were conducted with house dust allergen (Der p 1) standards obtained from the enzyme linked immunosorbent assay (ELISA) kit (Indoor Biotechnologies, Inc., Charlottesville, VA), and with H1N1 viruses (inactivated) received from Jiangsu Center for Diseases Prevention and Control (Jiangsu, China).

qPCR Experiments. In addition to the nanowire sensing, the collected virus aerosol samples used for the nanowire sensing were also analyzed using quantitative polymerase chain reaction (qPCR). The air samples were extracted for RNA by Tiangen RNA extraction kit (Tiangen, Beijing) following the manufacturer instructions. The RT-PCR experiments for airborne influenza A H3N2 virus samples were performed using the influenza H3N2 detection kit (BioPerfectus Technologies, Shanghai) under the conditions described by the manufacturer: 50°C (30 min, RT-PCR), 95°C (5 min, hold), and (95°C (10 s), 55°C (40 s))₄₀. The reaction mixture ($25 \mu\text{L}$) included RT-PCR

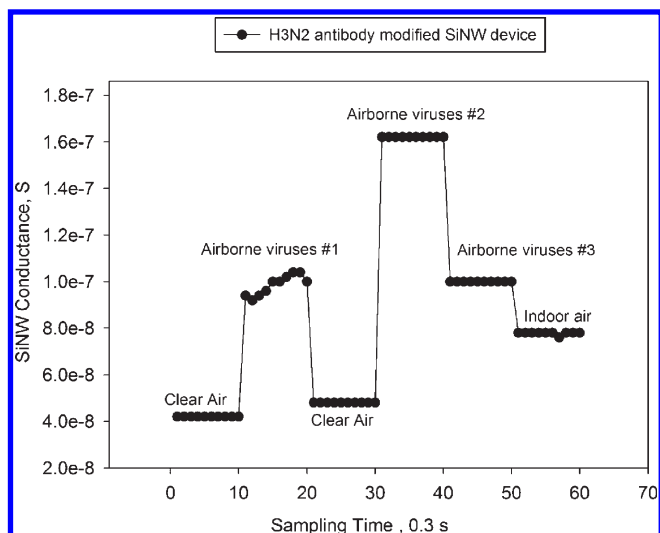


Figure 3. Real-time monitoring of airborne influenza H3N2 viruses using antibody modified SiNW devices; the airborne influenza virus samples, clean air (inside biological safety cabinet), and indoor air samples were collected into the liquid reservoir and delivered alternately to the nanowire sensor device through a microfluidic channel and a peristaltic pump; nanowire conductance levels vs time were monitored in a real-time manner using a preamplifier and a lock-in amplifier; nos. 1, 2, and 3 indicate three independent tests with airborne influenza A H3N2 viruses; the discrete changes in conductance levels for different samples were statistically significant (p -value < 0.001); qPCR tests indicated the virus concentrations in air sample nos. 1, 2, and 3 were below the detection limits (Figure 4).

reaction buffer ($7.5 \mu\text{L}$), Enzyme mix ($5 \mu\text{L}$), $4 \mu\text{L}$ of primers (400 nM) and probe (200 nM), Rnase free H_2O ($3.5 \mu\text{L}$), and sample RNA ($5 \mu\text{L}$). The influenza A H3N2 virus standards (9.8×10^8 gene copies/ μL) were obtained from Jiangsu Center for Diseases Prevention and Control (Jiangsu, China). The standards were serially diluted to 10^7 , 10^6 , 10^5 , 10^4 , 10^3 gene copies/ μL . The virus concentrations in the air samples were quantified when compared to the amplification curves of the virus standards.

Statistical Analysis. In this study, the nanowire conductance data (in discrete increases) obtained were not normally distributed, and the paired t test component from SigmaPlot 10.0 was used to analyze the differences. For qPCR tests, the air samples collected under a specific condition were pooled together to a total volume of 2 mL , and accordingly a statistical analysis is not applicable.

RESULTS AND DISCUSSION

When conducting the airborne virus sensing experiments, the influenza A H3N2 viruses were being continuously aerosolized into the chamber using the Collision nebulizer as shown in Figure 1. The airborne influenza A viruses were then collected using the electrical air sampler and delivered continuously onto the electronically addressable nanowire sensor devices via the microfluidic channel at a controlled flow rate of $0.4 \text{ mL}/\text{min}$. As illustrated in Figure 1, the nanowire conductance vs time data were recorded in a real-time manner using a preamplifier and a lock-in amplifier. In this work, alternate deliveries of clean air samples, indoor air samples and airborne virus samples were performed to investigate the specific detection of the airborne

viruses. Figure 3 shows the real-time airborne influenza A H3N2 virus sensing results using NWFET devices. As observed in Figure 3, when the H3N2 virus antibody-modified nanowire device was flowed through by the clean air samples collected inside of a class II biological safety cabinet, the conductance levels (10 measurements) of the nanowire device remained at $(4-5) \times 10^{-8} \text{ S}$. The conductance level was slightly increased up to $8 \times 10^{-8} \text{ S}$ when the collected indoor air samples were delivered to the nanowire sensor device. This slight increase in conductance level was likely caused by the nonspecific physical contact/binding that possibly occurred between the nanowire surface and substances in the indoor air samples collected. However, when the airborne H3N2 viruses were collected and delivered to the nanowire sensor device, the conductance levels were observed to substantially increase up to $1.6 \times 10^{-7} \text{ S}$ for the air sample no. 2 as shown in Figure 3. The conductance levels (10 measurements) for the airborne virus sample nos. 1 and 3 were observed around $1.0 \times 10^{-7} \text{ S}$, which was also discretely higher than those of the indoor air samples as observed in Figure 3. The signal-to-noise ratio was shown up to 4 for air sample no. 2. The results in Figure 3 indicated that whenever there were virus particles in the collected air samples flowed through the nanowire sensor device, the conductance levels of the nanowire devices would undergo a discrete change, higher than those caused by clean or indoor air samples, in a real-time manner, typically within seconds. The response time from airborne virus sampling, delivery, to the detection signal recording was observed to typically last about 1–2 min in this work. This time scale is lower than those of many available biological aerosol detection methods. The conductance level variations observed in Figure 3 were partially due to the variations of virus concentrations in the air samples collected. As observed in Figure 4, qPCR tests showed that the airborne virus concentrations in the air samples (clean air, indoor air, virus sample nos. 1, 2, and 3) were found below the detection limits of qPCR, although distinct FET responses were observed. In contrast, H3N2 virus standards (9.8×10^8 , 10^7 , 10^6 , 10^5 gene copies/ μL) and the positive control (1.8×10^4 gene copies/ μL) were efficiently amplified with cycle threshold (Ct) values ranging from 15 to 35 as seen in Figure 4. The observation with air samples would be likely due to either lower levels of the airborne virus concentrations or the virus losses during the tubing transport.

In a previous work, detection of single viruses was demonstrated with a conductance change of 10 nS corresponding to a single virus binding event observed using an optical microscope.¹² However, for qPCR, it was suggested that 10–100 gene copies can be achieved only provided that appropriate steps to mitigate inhibition have been taken, and the cell lysis and DNA purification steps in sample processing are efficient.¹⁶ Nested qPCR was shown to be able to further lower such detection limits through second round amplification of PCR products.^{17,18} However, the major advantage of a nanowire sensor for bioaerosol sensing is its shorter response time (seconds) compared to several hours for qPCR experiments. In the previous study, an average duration of $1.1 \pm 0.3 \text{ s}$ was observed to cause discrete conductance changes using both electrical and optical measurements.¹² Here, a rapid change of the conductance level was also observed within seconds upon the sample delivery. In our study, the delivered indoor air samples could contain diverse forms of biological particles including bacteria, fungi, allergens, endotoxins and other particles of biological origins. When the influenza A

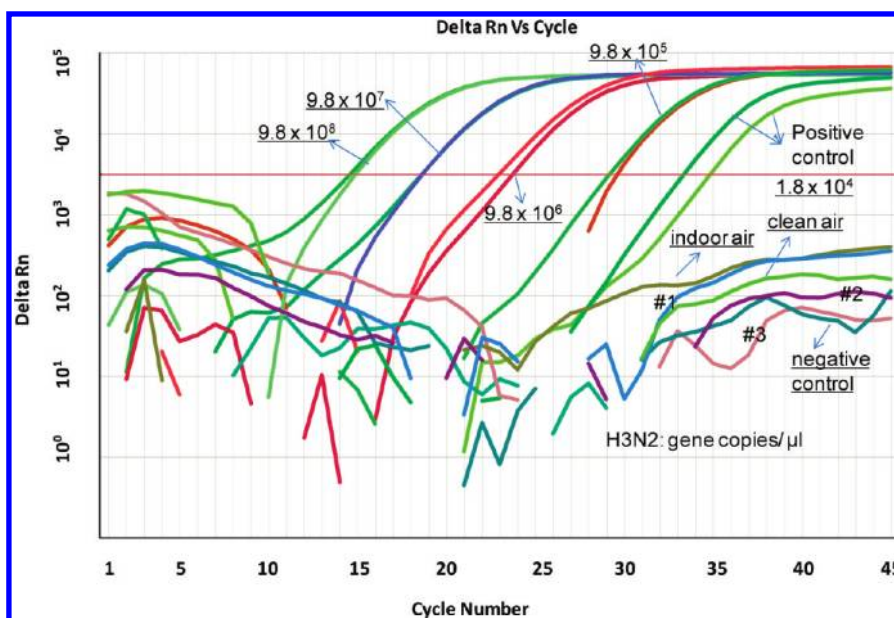


Figure 4. qPCR amplification of influenza H3N1 viruses in clean air, indoor and aerosolized samples detected using the silicon nanowire field effect transistor (SiNW-FET) shown in Figure 3; DI water was used as the negative control, and the positive control has a concentration of 1.8×10^4 gene copies/ μL ; virus standard concentrations were 9.8×10^8 , 9.8×10^7 , 9.8×10^6 , and 9.8×10^5 gene copies/ μL ; qPCR tests were performed at cycle conditions: 50°C (30 min, RT-PCR), 95°C (5 min, hold), and (95°C (10 s), 55°C (40 s))₄₀.

H3N2 virus antibody functionalized nanowire device was flowed through by a mixture of such biological particles along with other possible chemicals from the indoor environment, the conductance level of the sensor remained up to 2 times lower than the conductance level caused by the virus flow (no. 2) as observed in Figure 3. In addition, indoor air samples with longer sampling time (collecting 360 L of air into 20 mL water), that is, higher aerosol particle concentration, were also tested, and similar results were also obtained. The difference between indoor air and H3N2 virus samples indicates that specific binding of influenza A H3N2 viruses to the antibodies immobilized on the nanowire surface took place. This on the other hand also suggests that the airborne virus sensing system developed here could be applied to the real world environments as a result of the minor influence of indoor air.

In this study, we have characterized the FET's response and selectivity using standard H3N2 and H1N1 viral concentration levels as shown in Figure 5. As observed in Figure 5 (A), H3N2 virus concentration levels of $10^4, 10^5, 10^6/\mu\text{L}$ corresponded to the conductance levels of $(8, 9.6, 11.4) \times 10^{-8}\text{ S}$, respectively, for the device used. As observed in Figure 5 (A), a 10-fold increase in virus concentration resulted in an average $\sim 20\%$ increase in conductance level. However, due to the fabrication limitation of FET devices, such quantitative relationship could vary with sensor chips. However, use of standards and negative controls could calibrate a specific FET device before use. Besides, the H3N2 antibody modified FET sensor device was also tested by the delivery of house dust allergens (Der p 1) with concentration levels: 0.4 and 4 ng/mL (very high levels if transferred from the airborne state) to the nanowire sensor device in this study. As observed in Figure 5 (A), a 10-fold increase in Der p 1 concentration resulted in about $\sim 5\%$ increase in FET response. In addition, the selectivity of the H1N1 antibody modified nanowire sensor was also tested using H3N2 and H1N1 viruses as shown in Figure 5 (B). As observed in the figure, different

H1N1 virus concentration levels resulted in discretely different sensor (H1N1 antibody modified) responses, while the use of H3N2 viruses resulted in similar low FET responses regardless of concentration levels. The results shown in Figure 5 demonstrated the sensing selectivity of a specific antibody modified nanowire FET device. The sensitivity of the FET device could be influenced by many factors such as antibody concentration, stochastic binding kinetics and nonspecific touching and binding. Before use, a FET device should be calibrated with standards, buffer, and controls due to the FET fabrication variations.

To further quantify and define the relationship between the conductance levels of the nanowire devices and the virus concentrations in addition to those presented in Figure 5, qPCR tests were performed for H3N2 viruses in the air samples that were collected and used for the nanowire sensing. For this purpose, the airborne virus samples collected were directly pipetted onto the sensor device. Figure 6 shows the FET responses by different airborne influenza A H3N2 virus samples. As observed in Figure 6, the H3N2 antibody functionalized nanowire device used in this experiment was shown to have a baseline conductance level of around 1 nS (sometimes 2 nS). When the airborne virus samples (nos. 1, 2, and 3) of $5\mu\text{L}$ were added onto the nanowire sensor, the conductance increased sharply above 5 nS. When DI water (Millipore) was added onto the sensor device, the nanowire conductance was observed to increase slightly (around 2 nS). When high concentration virus samples (nos. 4, 5, and 6) were added onto the nanowire sensor device, their conductance levels were observed to increase to 15–25 nS as observed in Figure 6. The signal-to-noise ratio was observed up to 5 for the air sample no. 4. The air sample no. 4 had the highest conductance level as observed in Figure 6. qPCR results, as shown in Figure 7, indicated that no. 4 virus sample also had the highest virus concentration, followed by nos. 5 and 6. Compared to the virus standard curves shown in Figure 4, the air sample no. 4 corresponded to a concentration of 4×10^5 gene copies/ μL ,

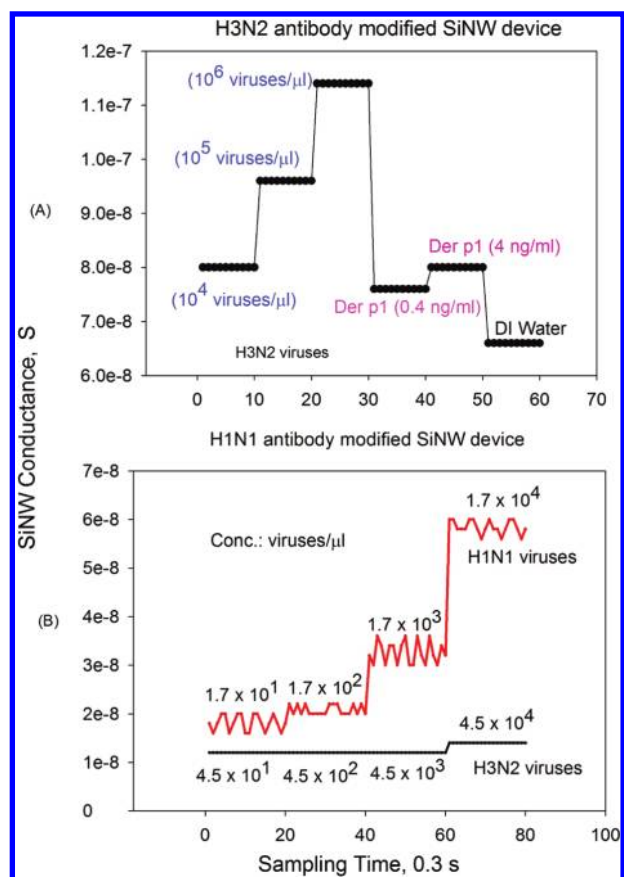


Figure 5. (A) Specific binding of H3N2 antibodies with H3N2 viruses, and nonspecific binding with Der p 1 allergens; The influenza A H3N2 virus concentrations tested here were 10^4 , 10^5 , and 10^6 viruses/ μ L; the Der p 1 allergen concentrations used were 0.4 and 4 ng/mL; (B) Specific binding of H1N1 antibodies with H1N1 viruses, and nonspecific binding with H3N2 viruses; the virus and allergen samples (5μ L) were pipetted directly onto the nanowire sensor.

while for other air samples their concentrations levels remained similar at $2^{-5} \times 10^4$ gene copies/ μ L. The negative control (DI water) had a Ct value of 34, below the detection limit of qPCR. The results from qPCR shown in Figure 7 corresponded well to those demonstrated by the nanowire sensing shown in Figure 6. Overall, higher influenza A virus concentrations in the air samples corresponded to higher conductance levels detected by the nanowire sensing as shown in Figure 6. After the virus sensing experiments, some viruses would remain on the sensor area without being washed off when the clean air samples and/or DI water were flowed through. This could help explain that the conductance level did not return to baseline after the virus sensing tests as shown in Figure 3 and Figure 6. For low level of H3N2 viruses, certainly there is a noise-to-signal ratio threshold only above which a positive signal could be obtained. This problem is common to all antibody based analytical techniques such as ELISA. The detection limit of the system developed here depends on many factors, including the microflow rate through the microfluidics, environmental pollutant matrix, the concentration of the antibody used to coat the nanowire, and the stochastic binding kinetics.

To further investigate the dependence of the silicon nanowire sensing on the virus concentration, different sampling voltages were investigated for the detection system shown in Figure 1.

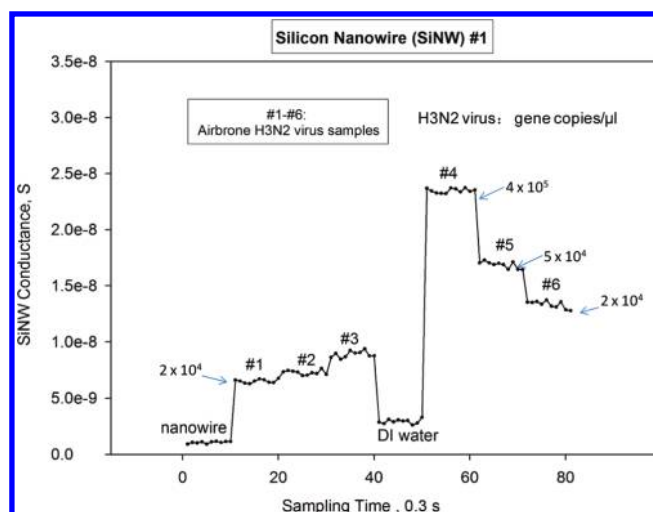


Figure 6. Use of silicon nanowire field effect transistor (SiNW-FET) for real-time detection of airborne influenza H3N2 viruses (first experiment): air sample nos. 1–6 were first collected into the liquid reservoir at a 20 kV sampling voltage and further delivered into 2 mL tubes; 5μ L of each air sample was pipetted directly onto the nanowire sensor; the nanowire conductance levels were monitored in a real-time manner; the discrete changes in conductance levels for different samples were statistically significant (p -value < 0.001); the virus concentrations in the air samples were quantified using qPCR (Figure 7).

The airborne influenza A H3N2 virus samples were collected at different sampling voltages, and 5μ L of each air sample collected was pipetted directly onto the nanowire sensor device. At the same time, the virus concentration levels for the same air samples collected were quantified using qPCR. Figure 8 and SI Figure S3 show the nanowire device sensing and qPCR results, respectively. qPCR results indicated that in most cases when the applied sampling voltage was increased the virus concentrations in the air samples were found to increase as shown in SI Figure S3, ranging from 1.8×10^4 to 7×10^7 gene copies/ μ L. The signal-to-noise ratios were observed from 100 to 200 for the air samples collected as shown in Figure 8. Increasing sampling voltage induced stronger electrical field strength, which in turn resulted in higher physical collection efficiencies for the airborne virus particles. As observed in Figure 8 and SI Figure S3, the increases in virus concentrations induced increases in the conductance levels of the nanowire devices. The variations in conductance levels of the nanowire devices for the samples collected with the same sampling voltage might be also due to the variations in the collection efficiencies of the electrostatic air sampler or the variations in airborne virus concentrations generated. Nonetheless, there were some discrepancies observed between the nanowire sensing and the qPCR tests, which were likely due to the antibody receptor and virus binding kinetics, nonspecific physical binding of the nanowire sensing devices, and/or relevant inhibition and amplification efficiency problems associated with the qPCR tests. In addition, DNA extraction efficiency variation might have also played a role. The discrepancies observed between different voltages could be also due to the virus losses during the tubing transport as aforementioned.

The work here is expected to lead to innovative methods for real-time monitoring of biological aerosols by integrating the technologies in different disciplines. The sensing system here has been demonstrated to have the capability to monitor the airborne

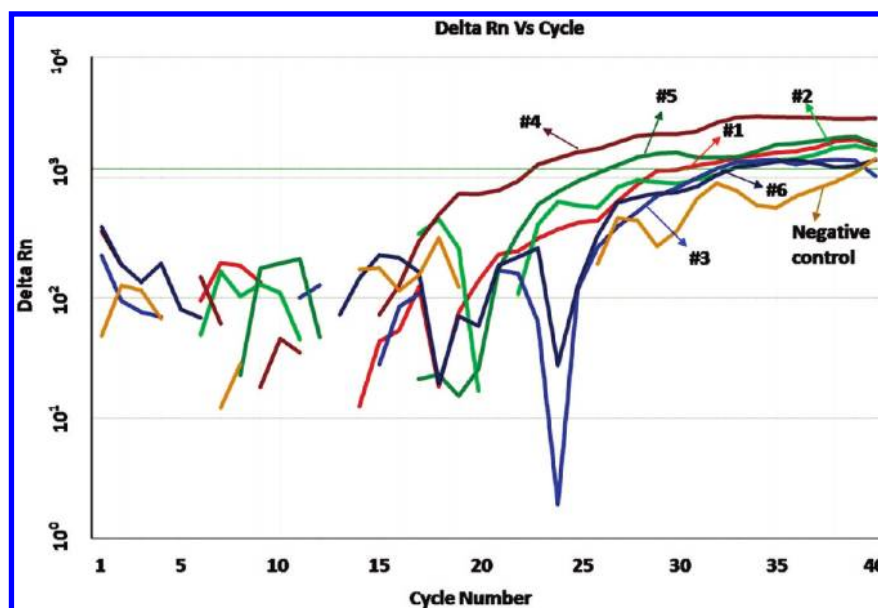


Figure 7. qPCR amplification of airborne influenza H3N2 viruses in the samples detected using silicon nanowire field effect transistor (SiNW-FET) shown in Figure 6; DI water was used as the negative control, qPCR tests were performed at cycle conditions: 50 °C (30 min, RT-PCR), 95 °C (5 min, hold), and (95 °C (10 s), 55 °C (40 s))₄₀.

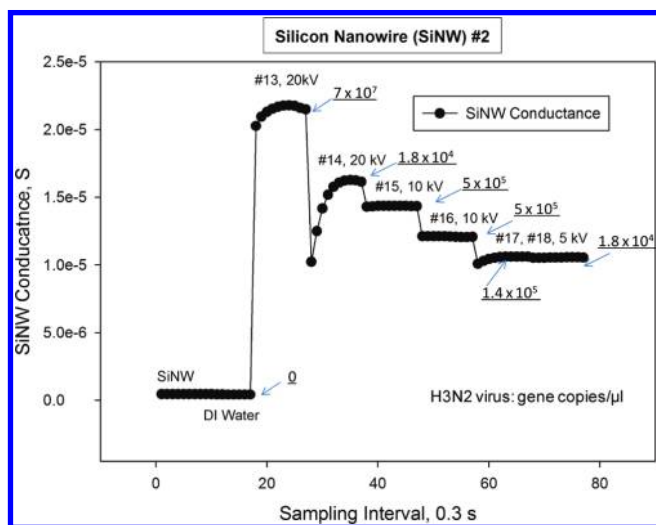


Figure 8. Use of silicon nanowire field effect transistor (SiNW-FET) for real-time detection of airborne influenza H3N2 viruses (second experiment); air sample nos. 13–18 were collected into the liquid reservoir by the electrical air sampler at different sampling voltages: 20, 10, and 5 kV, and further delivered into 2 mL tubes; 5 μ L of each air sample was pipetted directly onto the nanowire sensor; the nanowire conductance levels vs time were monitored in a real-time manner; the discrete changes in conductance levels for different samples were statistically significant (p -value < 0.001); the virus concentrations in the air samples were quantified using qPCR (SI Figure S3).

presence of influenza A viruses in a real-time manner, typically from 1 to 2 min. This response time scale is lower than those of many available bioaerosol sensing systems. Results in this study indicated that the system could detect the airborne influenza A H3N2 viruses air with a concentration of 10^4 viruses/L or lower. The system developed here can be customized to detect other types of biological aerosols by using target-specific antibodies. In addition, it is possible that hundreds of sensor arrays with

different antibody receptors can be spotted on the chip carrier at the same time for simultaneous detection of bioaerosols of different origins. Certainly, the concept of the system developed here is not just limited to the silicon nanowire sensor, but also many other available biosensor technologies such as DNA microarray¹⁹ and carbon nanotube field effect transistor²⁰ technologies which can also be adapted for label-free real-time detection of bioaerosols following the system presented in Figure 1. In addition, the system was tested with our wireless module shown in SI Figure S4 which transmits the silicon nanowire conductance data remotely via an antenna and the existing network. The display of nanowire conductance data on remote platforms such as cell phone and computer was successfully demonstrated in our laboratory. In this study, a sampling flow rate of 5 L/min was used. In future, high volume aerosol-to-hydrocol air sampling technique can be integrated. Development of robust, stable and specific sensor receptor will go a long way toward the practical application and efficiency of the system investigated here. Undesirably, the system developed here could be negatively impacted by the nonspecific physical binding, cross-reaction problems common to antibody-based detection methods, environmental pollutant matrix in the air samples, and also the lifetime of the antibody when exposed to environmental conditions. Common to other antibody-based detection methods, the system here cannot differentiate between dead and live viruses. Here, we have demonstrated a practical airborne virus sensing platform by integrating air sampling, microfluidics and FET devices. Further improvements in each of the elements could extend the sensing platform to real world applications, for example, for monitoring biological threats in military bases, public civilian establishments, and healthcare facilities.

■ ASSOCIATED CONTENT

Supporting Information. Additional information as noted in the text. This material is available free of charge via the Internet at <http://pubs.acs.org>.

AUTHOR INFORMATION

Corresponding Author

*Phone: +86 010 6276 7282 (M. Y.); +86 01062757789 (X. G.); +86 01062754789 (T. Z.). E-mail: yao@pku.edu.cn (M. Y.); guoxf@pku.edu.cn (X. G.); tzhu@pku.edu.cn (T. Z.).

Author Contributions

F.S, M.T., and Z.W. contributed equally to the work.

ACKNOWLEDGMENT

This study was supported by the National High Technology Research and Development Program of China (Grant 2008AA062503), and National Science Foundation of China (Grant 20877004, 21077005 and 20833001).

REFERENCES

- (1) Guan, Y.; Zheng, B. J.; He, Y. Q. X.; Liu, L.; Zhuang, Z. X.; Cheung, C. L.; Luo, S. W.; Li, P. H.; Zhang, L. J.; Guan, Y. J.; Butt, K. M.; Wong, K. L.; Chan, K. W.; Lim, W.; Shortridge, K. F.; Yuen, K. Y.; Peiris, J. S. M.; Poon, L. L. M. Isolation and characterization of viruses related to the SARS coronavirus from animals in Southern China. *Science* **2003**, *302*, 276–278.
- (2) Stone, R. Combating the bird flu menace, down on the farm. *Science* **2006**, *311*, 944–946.
- (3) Enserink, M. How devastating would a smallpox attack really be? *Science* **2002**, *296*, 1592–1592.
- (4) Tobias, H. J.; Schafer, M. P.; Pitesky, M.; Ferguson, D. P.; Horn, J.; Frank, M.; Gard, E. E. Bioaerosol mass spectrometry for rapid detection of individual airborne *Mycobacterium tuberculosis* H37Ra particles. *Appl. Environ. Microbiol.* **2005**, *71*, 6086–6095.
- (5) Sengupta, A.; Brar, N.; Davis, E. J. Bioaerosol detection and characterization by surface-enhanced Raman spectroscopy. *J. Colloid Interface Sci.* **2007**, *309*, 36–43.
- (6) Chen, P. S.; Li, C. S. Bioaerosol characterization by flow cytometry with fluorochrome. *J. Environ. Monit.* **2005**, *7*, 950–959.
- (7) Ho, J.; Spence, M.; Fisher, G. *Detection of BW Agents: Dugway Trinational BW Field Trial 20–30 October 1993, Dugway, Utah, Mobile Aerosol Sampling Unit Data Analysis*, Defense Research Establishment Suffield Report 619, 1995.
- (8) Agranovski, V.; Ristovski, Z.; Hargreaves, M.; Blackall, P. J.; Morawska, L. Real-time measurement of bacterial aerosols with the UVAPS: performance evaluation. *J. Aerosol Sci.* **2003a**, *34*, 301–317.
- (9) National Research Council. *Sensor Systems for Biological Agent Attacks: Protecting Buildings and Military Bases*; The National Academies Press: Washington, DC, 2005.
- (10) Agranovski, V.; Ristovski, Z.; Hargreaves, M.; Blackall, P. J.; Morawska, L. Performance evaluation of the UVAPS: influence of physiological age of airborne bacteria and bacterial stress. *J. Aerosol Sci.* **2003b**, *34*, 1711–1727.
- (11) Cui, Y.; Wei, Q.; Park, H.; Lieber, C. M. Nanowire nanosensors for highly sensitive and selective detection of biological and chemical species. *Science* **2001**, *293*, 1289–1292.
- (12) Patolsky, F.; Zheng, G.; Hayden, O.; Lakadamyali, M.; Zhuang, X.; Lieber, C. M. Electrical detection of single viruses. *Proc. Natl. Acad. Sci. U. S. A.* **2004**, *101*, 14017–14022.
- (13) Patolsky, F.; Zheng, G.; Lieber, C. M. Fabrication of silicon nanowire devices for ultrasensitive, label-free, real-time detection of biological and chemical species. *Nat. Protoc.* **2006**, *1*, 1711–1724.
- (14) Yao, M.; Chon, K. H.; Zhen, S. Integration of technologies for constant monitoring of exposure [E-Letter]. *Science*, June 14, **2007**, <http://www.sciencemag.org/cgi/eletters/316/5825/695>.
- (15) Whitesides, G. M.; Ostuni, E.; Takayama, S.; Jiang, X.; Ingber, D. E. Soft lithography in biology and biochemistry. *Annu. Rev. Biomed. Eng.* **2001**, *3*, 335–373.
- (16) Peccia, J.; Hernandez, M. Incorporating polymerase chain reaction-based identification, population characterization, and quantification of microorganisms into aerosol science: A review. *Atmos. Environ.* **2006**, *40*, 3941–3961.
- (17) Perrott, P.; Smith, G.; Ristovski, Z.; Harding, R.; Hargreaves, M. A nested real-time PCR assay has an increased sensitivity suitable for detection of viruses in aerosol studies. *J. Appl. Microbiol.* **2009**, *106*, 1438–1447.
- (18) Stark, K. D. C.; Nicolet, J.; Frey, J. Detection of *Mycoplasma hyopneumoniae* by air sampling with a nested PCR assay. *Appl. Environ. Microbiol.* **1998**, *64*, 543–548.
- (19) Schena, M.; Shalon, D.; Davis, R. W.; Brown, P. O. Quantitative monitoring of gene expression patterns with a complementary DNA microarray. *Science* **1995**, *270*, 467–470.
- (20) So, H. M.; Won, K.; Kim, Y. H.; Kim, B. K.; Ryu, B. H.; Na, P. S.; Kim, H.; Lee, J. O. Single-walled carbon nanotube biosensors using aptamers as molecular recognition elements. *J. Am. Chem. Soc.* **2005**, *127*, 11906–11907.
- (21) Tan, M.; Shen, F.; Yao, M.; Zhu, T. Development of an automated electrostatic sampler (AES) for bioaerosol detection. *Aerosol Sci. Technol.* **2010**, *45*, 1154–1160.